Laser and Particle Beams (2005), *23*, 357–363. Printed in the USA.
Copyright © 2005 Cambridge University Press 0263-0346/05 $16.00
DOI: 10.1017/S0263034605050512

On Stark broadening as a tool for diagnostics of high density plasmas*

C. STEHLÉ,[1] M. BUSQUET,[1] D. GILLES,[2] AND A.V. DEMURA[3]
[1]Laboratoire de l'Univers et de ses Théories, UMR 8102 du CNRS, Meudon, France
[2]Commissariat à l'Energie Atomique, Bruyères-le-Châtel, France
[3]Hydrogen Energy & Plasma Technology Institute, State Research Center of Russian Federation, Moscow, Russia

(RECEIVED 30 November 2004; ACCEPTED 6 January 2005)

Abstract

We present the current status-of-the-art in Stark broadening theory as a theoretical basis for diagnostics of low temperature plasmas in gas discharges, and of high temperature laser produced or z-pinch dense plasmas. The diagnostics abilities vary depending on the parameters of the gas discharges, or on the range of intensity, and duration of the laser or z-pinch pulses. In the case of high temperature plasmas, besides the conventional diagnostics based on the Stark broadening, the contemporary possibilities of UV and XUV interferometry for plasma density measurements and of tomography reconstruction of the macroscopic gradients of temperature and densities in laser produced plasmas are discussed.

Keywords: Dense plasma diagnostics; Interferometry; Laser; Stark broadening; z-pinch

1. INTRODUCTION

The effect of Stark broadening (SB) in plasmas is one of the most effective tools to determine dense plasma properties experimentally, especially for beam plasma interaction experiments with intense beams of photons and particles (Loboda *et al*., 2000; Politov *et al*., 2000; Magunov *et al*., 2003; Hasegawa *et al*., 2003; Ying *et al*., 2003). It is associated with the idea that electric microfield acting on the test particles is the sum of all the electric fields created by the perturbing ions, in the scale of distances at which the quasi-neutrality condition is not fulfilled (see Demura & Gilles, 2004). Hydrogen-like and helium-like lines are the most sensitive to SB, but for practical reasons, we restricted our discussion to hydrogen-like lines. The Stark effect is also responsible for the splitting of spectral lines in several components. The SB of Hydrogen-like lines were proposed for diagnostic of the plasma density after the pioneer work of Holtsmark (1919), where only the Coulomb electric fields of point ions were considered and assumed to be random and static. The half width of the Stark broadened line is determined by the microfield probability distribution function (PDF). The first tabulation of the Stark profiles of the hydrogen spectral line was done by Underhill and Waddell (1959) in the quasi-static approximation for ions with the help of Holtsmark PDF, while the SB by electrons was neglected. Later this simple concept was developed in order to take into account (1) the two types of charged particles in plasma-ions and electrons; (2) the microfield time dependence; (3) the microfield non-uniformity which is connected to the departure from the dipole approximation of the interaction potential between the radiator and the plasma particles; and other specific effects connected to each experimental cases. The introduction of the impact and quasi-static approximations (Griem, 1974) was the simplest of indirectly accounting for the time microfield dependence. This approach, when the SB by electrons is described in the impact approximation while the SB by ions, in the quasi-static approximation with the help of PDF, was reflected in the hydrogen lines tables (Kepple & Griem, 1968), named thereafter KG68. However, the transition of the SB by electrons from the impact to the quasi-static regime in the wings of spectral lines was neglected in the KG68 approach. This transition was described in the frame of the so-called unified theory using the one electron approximation in Vidal *et al*. (1973), named thereafter VCS73. The corresponding tables Stark profiles of Hydrogen lines are presented in VCS73.

The common starting point for the calculation of the line shapes begins with the Fourier transform of the average Liouville evolution operator $U(t)$. The radiation intensity of

---

Address correspondence and reprint requests to: Chantal Stehlé, Laboratoire de l'Univers et de ses Théories, UMR 8102 du CNRS, Observatoire de Paris, 5 Place J. Janssen, 92195 Meudon, France. E-mail: chantal.stehle@obspm.fr

*This paper was presented at the 28th ECLIM conference in Rome, Italy the optical transition between two groups of atomic levels, denoted by i, i', and f, f', is given by

$$I(\omega) = \frac{1}{\pi}\,\mathrm{ReTr}\int_0^\infty \mathrm{e}^{i\omega t}\langle\langle d^*|U(t)|d\rho\rangle\rangle dt, \tag{1}$$

where d and ρ are the dipole and the density matrix operators for the system. For the last quantity, one usually chooses the diagonal equilibrium density matrix operator ρ_0 for the unperturbed system (that is, without the effects of the surrounding plasma charges). The average trace is taken over the free atom (or ion) Liouville states contributing to the optical transition. As the initial eigenstates i, i' of the optical transition are very close in energy, then the diagonal equilibrium density operator may be considered as constant and deleted in Eq. (1). In the quasi-static approximation for the ions and impact approximation for the electrons, the plasma average in Eq. (1) is expressed in terms of ion probability field distribution W (F). Using now for the calculation of the eigenstates of the radiator, perturbed by the constant field F, and assuming for simplicity that the impact operator ϕ is diagonal, the intensity could be expressed as:

$$I(\omega) = \frac{1}{\pi}\,\mathrm{ReTr}_{if}\int_0^\infty dF\, W(F) I_{if}(F)[i(\omega - E_{fi}(F)/\hbar) + \phi_{fi}], \tag{2}$$

where I_{if} is the individual component intensity from i to f and $E_{\mathrm{fi}} = E_{\mathrm{f}} - E_{\mathrm{i}}$ is the transition energy. The first more general description of SB in terms of time dependent microfields was given in the frames of the model microfield method (MMM) (Frisch & Brissaud, 1971; Brissaud *et al.*, 1976). This model recovers the quasi-static and impact limits of SB by electrons (Stehlé, 1990).

The aim of this paper is to summarize the present status in SB theory in plasmas as a basis of the electronic density diagnostics. We start with the case of low temperature and low density gas discharges, where SB is widely used as a diagnostics, and performances, which can be obtained in these plasmas. Then we present the experimental constraints for high density plasmas and the SB possibilities in these more complex situations. We will also focus on ICF plasmas obtained on lasers or Z pinches facilities (Woolsey *et al.*, 1997; Stygar *et al.*, 2004; Bailey *et al.*, 2004). However, it is important to check SB theoretical predictions in some experiments where other diagnostic can simultaneously provides determination of density. In this context, the contemporary abilities of the UV and X-ray plasma interferometry are very promising (Hammarsten *et al.*, 2004; Zeitoun *et al.*, 2004). The SB diagnostic is also a part of more complicated methods such as polarization spectroscopy (Fujimoto & Kazansky, 1997; Hakel *et al.*, 2004), magnetic polarizer (Mathys *et al.*, 2000), and absorption and fluorescence spectroscopy (Gouveia *et al.*, 2003; Regan *et al.*, 2002; Chambers *et al.*, 2002; Rosmej *et al.*, 2003).

2. LOW TEMPERATURE PLASMAS

In this section, we present the application of SB to plasmas with electron temperature $T_{\mathrm{e}} \sim 1$ eV and plasma electron density $N_{\mathrm{e}} \sim 10^{18}$ cm^{-3}. Many experimental devices are concerned: plasma torches, discharges, laser induced plasmas, and inductively coupled plasmas. Such plasmas are mostly quiet, uniform, and with long time duration. This allows an accurate spectroscopic measurement of Hydrogen lines. Besides that, electronic density may be measured independently by laser interferometry, allowing a validation of the theories and their further use as an autonomous diagnostic.

A major step of improvement was achieved with the inclusion of ion dynamics in the line broadening theories, starting with the MMM theory. MMM (Seidel, 1977) first gave the order of magnitude of the neutral hydrogen Lyman-α half width measured in the stabilized arcs (Grützmacher & Wende, 1977), with a value 2.5 times larger than KG68 and VCS73 ones! The recent extensive MMM tables are available in Stehlé & Hutcheon (1999).

The first direct computer simulation of SB in the time dependent microfield was performed in the approximation of the straight classical trajectories of the perturbing particles. This model, hereafter called computer simulation along straight trajectories (CSST), gives in principle a better description of ion dynamics than MMM. The CSST tables for the corresponding Hydrogen lines are presented in Gigosos and Cardenoso (1996), and for the recent developments with the joint simulations of the ion and electron microfields (Gigosos *et al.*, 2003). However, the CCST model neglects correlations between "field" particles, important for high density, in principle, are included in MMM. On the basis of KG68, VCS73, MMM, and CSST theories, comparison of the measured and the calculated Stark profiles of hydrogen lines yields an accuracy better than 20% for the density determined for uniform isotropic low temperature plasma of gas discharges without self-absorption. The recent comparison of the full Balmer Stark profiles of H_α, H_β, and H_γ given by experiment and by MMM and VCS73 is shown in Figure 1 (Acon, B.W., Stehlé, C. & Montaser, A., 2004, private communication). Using the full line shapes, the electronic densities are determined to be, respectively (in cm^{-3}): 3.0×10^{13} (3.5×10^{14}) for H_α, 4.9×10^{13} (3.9×10^{13}), for H_β, 3.7×10^{13} (4.0×10^{13}) for H_γ using MMM and VCS (in brackets). The measurements were made in plasma torch inductively coupled plasma (ICP) radio-frequency discharge (Cai *et al.*, 1994). MMM computations were performed with $T_{\mathrm{e}} = T_{\mathrm{i}} = 10000$ K.

These theories are based on standard linear Stark effect, connected to dipole approximation. This linear effect gives the dominant contributions to the line shapes. But spectral line shifts (Nguyen *et al.*, 1986; Koenig *et al.*, 1988), quadrupole and higher order field effects start to affect the line shape at densities larger than 10^{17} cm^{-3}. In dense plasmas the dipole approximation becomes insufficient to

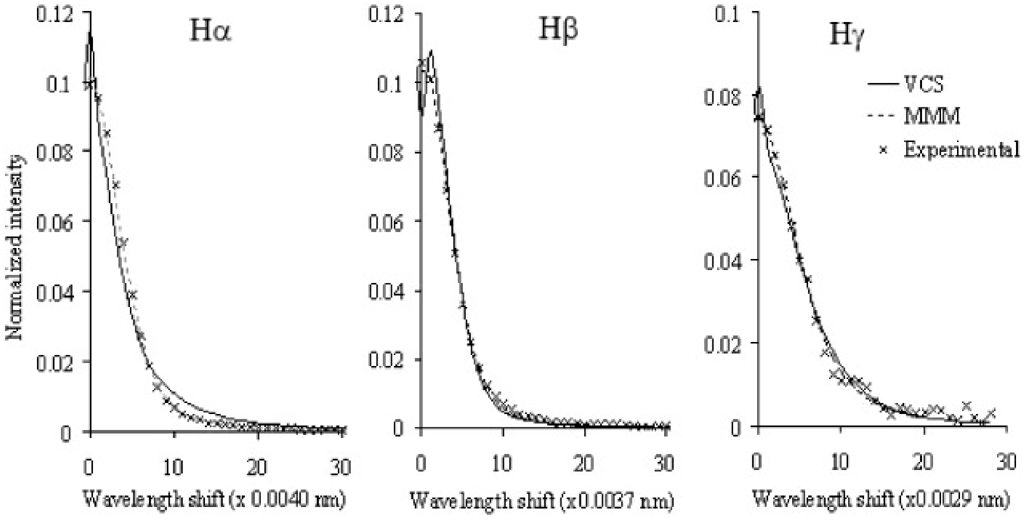

Fig. 1. Best fit of theoretical profiles compared to experimental profiles of Balmer lines recorded in an Helium ICP collected with a high-resolution Fourier transform spectrometer.

describe the interaction of the field particles with the radiator. However, the non-dipole interaction may be considered as a perturbation, so the problem can be solved in terms of the joint distribution function of microfield and its spatial derivatives (Demura & Sholin, 1975; Demura *et al*., 1995; Stehlé *et al*., 2000). Moreover, the MMM as the current CSST codes neglect the effects of the radiator motion using so-called μ-model, that considers only the radiator-perturbed relative motion operating with the reduced mass μ of this pair. The investigation of the effects of the radiator motion also could be done in some special versions of CSST. Although the inclusion of the radiator motion leads to the appearance of several qualitative effects, its overall influence on the Stark profile was found to be negligible.

Beside MMM, there are other indirect models for description of ion dynamics effects such as the frequency fluctuation model (FFM) (Talin *et al*., 1995) and the frequency separation model (FST) (Alexiou *et al*., 1997), that in fact are complementary to each other. As they are mostly used for ionic emitters, we present them in more details in the following section. The joint microfield distribution at the neutral or the charged points were recently studied in the Molecular Dynamics simulations of ions and electrons, which allows consider strongly coupled plasmas and the influence of the perturber-perturber correlations (Talin *et al*., 2003; Ferri *et al*., 2004). The Molecular Dynamics allows as well testing directly the applicability of μ-model in the ion dynamics depending on the plasma parameters.

All these lines may be and are already used for plasma diagnostic. Among them, the H_β is relatively insensitive to the ion dynamics (except for the line center dip). Thus, this line may be considered as a corner stone for the diagnostic of low temperature plasmas. The use of the line shape in the near line wings (Acon *et al*., 2001) allows the more precise determination of the electron density than using the half width value which is more sensitive to the continuum determination in the case of broad lines.

3. HIGH TEMPERATURE PLASMAS OF LASER TARGETS AND Z-PINCHES

In this section, we will consider plasmas of mid-atomic number ($10 < Z < 36$) obtained in high power installations (lasers or z-pinches), and more precisely having temperatures at least several hundred eV and densities around or larger than 10^{21} cm^{-3}. We also focused on Hydrogen and Helium lines.

The theoretical context for Stark profiles of the lines of Hydrogen-like ions is quite similar to the case of Hydrogen lines in low density plasmas. Among previous works summarizing the subject of X-ray spectroscopy application to laser targets and pinch plasmas it is worthy to refer to Boiko *et al*. (1980). The first scaling analysis of SB application for diagnostics of laser plasmas with highly charged ions was performed by Vinogradov *et al*. (1974) using the impact and quasi-static broadens approximations. Molecular dynamics simulations have shown later (Langer *et al*., 2003) that spectral line width of impurities in mixture—used to trace the plasma parameters—are dramatically increased by ion dynamics (Stamm *et al*., 1986) for typical laser plasmas conditions. The importance of ion dynamics is quite large for lines like Ly_α and He_α, but remains negligible for Ly_β and He_β lines, if one excludes the dip in the line center. The MMM and FFM are alternative methods to describe this effect. Although there are remarkable examples of spectra generated in the frames of FFM that fit well experimental data, it should be kept in mind that FFM operates with the artificial set of two level subsystems adjusted to fit the real static spectrum of the radiating system. The ion dynamics effects are modeled within FFM with an additional parameter—the mixing frequency which artificially couples the microfield substates. This frequency is a constant in FFM, independent of the microfield, contrarily to the MMM frequency jump. Thus, the transition region, which occurs in the line centre between the impact approximation and the quasi-static approximation, has a different variation with density and temperature. Furthermore, a constant mixing frequency prevents FFM from converging toward the quasi-static limit in the far line wings. This shortcoming is not found in the sophisticated kinetic method for charged radiators (Boercker *et al.*, 1987) where the mixing frequency is a function of the detuning from the line center. This theory, formulated for the one component plasma model, couples the plasma microfield statistics and the radiating ion velocity, and set the time integral of the field autocorrelation function to zero. It should be noted, that unlike the MMM, the FFM code could not be reproduced in this paper.

In ICF plasmas and in some other experiments, radiating impurities are introduced in the target for diagnostic purpose. In this case, the line shapes are sensitive to the plasma composition. This sensitivity is a consequence of both plasma ion dynamics and statistics effects in the field distribution functions (Iglesias *et al.*, 2000). They were demonstrated using Monte Carlo (Gilles, 1990; Potekhin *et al.*, 2002) and MMM methods (Gilles & Stehlé, 1994, 1995). However, this effect is relatively small for the Ly_β and He_β lines.

Another subtle effects is found when initial and final atomic levels are mixed by the plasma microfield and the non-diagonal elements of the density matrix (Eq. 1) has to be included in the calculation of the line profile, which means that SB entangles with kinetics (Anufrienko *et al.*, 1993; Kosarev *et al.*, 1997), in contrast to the usual assumption of a diagonal density matrix in SB (Griem, 1974). These phenomena are known in laser physics as the nonlinear interference effects (NIEF) (Rautian & Shalagin, 1991). It was found that the NIEF also strongly influences the X-ray lasers kinetics (Gasparian *et al.*, 1994). This may be generally neglected in a first approximation.

In strongly coupled plasmas, elegant molecular models were formulated to study the possibility of the formation of two-center (or molecular) transient configurations leading to the apparition of quasi-molecular satellites in the near line wings of Hydrogen-like ions (Leboucher-Dalimier *et al.*, 2001). However, experimentally these observations are extremely difficult to perform. Note also that small dips in the line wings can be generated by intense plasma waves such as those produced by the laser field (Oks, 1995).

More important are the effects of gradients of the microfields (Stehlé *et al.*, 2000) and of quadrupole and higher order field (Kilcrease *et al.*, 1993), which increase with density and lead to line asymmetries and line merging (Inglis & Teller, 1939). Among the 1s-np and 1 s^2–1 s-np series of the Hydrogen- and Helium-like ions, the Ly_β and He_β lines are only slightly affected by these perturbations, but still intense and thus well suited for diagnostic purpose.

For highly charged ions, SB presents other concerns, such as line shifts due to electron collisions (Nguyen *et al.*, 1986; Koenig *et al.*, 1988; Renner *et al.*, 2003). As integration along the line of sight includes different densities to which these shift are dependent, and can lead to apparent broadened and asymmetric profile. But regretfully, the various theoretical approaches differ considerably in the predicted shift values and their functional dependences on plasma parameters. In the absence of validated theories, the analytical expression of Nguyen *et al.* (1986) may be considered as a possible starting point.

One other difficulty, which is not directly related to the SB theory, is the contribution from the resolved and unresolved dielectronic satellites (as for example the Ly_β satellites 1s nl–3p nl), that inevitably transform the observable SB pattern in the red wing. The deconvolution of the satellites and the red wing would require a full processing for the population balance of the doubly and singly excited states. Thus analysis of the red wing profile of the parent lines may not provide an independent density measurement.

SB of dielectronic satellites from "hollow ions," which do not overlap with the parent line, were studied in details (Rosmej *et al.*, 2003). Suitable for temperature diagnostic through their intensities, these lines appear not to be suitable for density determination.

We will discuss now the experimental context. Laser produced plasmas are characterized by noticeable non-stationary, non-uniformity, and as a rule, large departure from LTE ionization equilibrium (Busquet *et al.*, 2003). This brings out complex interpretation of the observations, as probing one density and one temperature will never be achieved and time-resolved tomographic reconstruction is extremely difficult due to the small size of the rapidly varying plasma. However, an impressive reconstruction of temperatures (and densities in a lower extent) of an indirect drive target on the OMEGA laser was performed (Welser *et al.*, 2003) under few simplifying assumptions (such as isotropy or monotonic gradient, see Golovkin *et al.* (2002). A 1280 pinhole array associated with a flat multi-layered Bragg mirror provides monochromatic image (75 eV bandwidth) for each parent lines and their satellites. Genetic algorithm acting on the recorded intensities is used to set a few parameters describing the density and temperature profiles. The collisional radioactive model used for this reconstruction includes satellites, radioactive transport, and Stark profiles. SB is also used to add constraints on density from the time integrated spectrum, see Figures 3 and 5 in Welser *et al.* (2003). This deconvolution starts from detailed observed data and derives hydrodynamical quantities. In fact, analysis of the experiment would require as a complement to start from hydrodynamical code and through atomic modeling, radioactive transfer and line profile create synthetic spectral data.

In conclusion, in case of high temperature plasmas, we recommend to use of the blue wing of He_β or Ly_β lines in order to minimize ion dynamics effects, and avoid unresolved satellites. A quasi-static approach of the line shape will be a good first description. An accurate subtraction of the pseudo continuum is necessary, as it will cancel part of the observed asymmetry.

4. CONCLUSION

In summary, Stark broadening is widely used as a density diagnostic in low and high temperature plasma in various experimental settings. Improvement of the underlying theory is still in progress regarding line shift by electronic collisions, dielectronic satellites. . . . High resolution in space, time and spectra (possibly all at the same time!) will obviously allow better determination of local density and temperature. The deconvolution of the experimental spectra emitted by dense plasmas will benefit from post-processing by a full time-dependent collisional-radioactive model (CRM)—including radiation transfer—of a reliable hydrodynamic simulation (Busquet *et al*., 2004). Thus this CRM may require including NIEF (Anufrienko *et al*., 1993; Kosarev *et al*., 1997). In the recent experimental studies of dense laser plasmas, the SB diagnostics is used simultaneously with other density diagnostics in order to perform cross check on the plasma parameters as it was done for the classical studies of the gas discharge plasmas. In this respect the current development of the UV and X-ray interferometry is very appealing for increasing reliability of the SB diagnostic.

ACKNOWLEDGMENTS

The authors are indebted to B.W. Acon for providing the set of hydrogen data and for helpful suggestions. C. Stehlé acknowledges the support of Comité National Français d'Astronomie.

REFERENCES

Acon, B.W., Stehlé, C., Zhang, H. & Montaser, A. (2001). Stark-broadened hydrogen line profiles predicted by the model microfield method for calculating electron number densities. *Spectr. Chem. Acta*, **B 56**, 527–539.

Alexiou, S., Calisti, A., Gauthier, P., Klein, L., Leboucher-Dalimier, E., Lee, R.W., Stamm, R. & Talin, B. (1997). Aspects of Plasma Spectroscopy: Recent Advances. *J.Q.S.R.T.* **58**, 399–413.

Anufrienko, A.V., Bulyshev, A.E., Godunov, A.L., Demura, A.V., Zemtsov, Yu.K., Lisitsa, V.S. & Starostin, A.N. (1993). Nonlinear Interference Effects and Ion Dynamics in Kinetic Theory of Stark Broadening of Multiply Charged Ion Spectral Lines in Dense Plasmas. *Sov. Phys. JETP* **76**, 219–228.

Boiko, V.A., Vinogradov, A.V., Pikuz, S.A., Skobelev, I.Yu. & Faenov, A.Ya. (1980). X-ray spectroscopy of laser plasmas. In *Science and Technique Series, Radiotechnique* v. 2, ed. N.G. Basov, VINITI, Moscow (in Russian).

Bailey, J.E., Chandler, G.A., Slutz, S.A., Golovkin, S.A., Lake, P.W., MacFarlane, J.J., Mancini, R.C., Burris-Mog, T.J., Cooper, G., Leeper, R.J., Mehlhorn, T.A, Moore, T.C., Nash, T.J., Nielsen, D.S., Ruiz, C.L., Schroen, D.G. & Varnum, W.A. (2004). Hot Dense Capsule-Implosion Cores Produced by Z-Pinch Dynamic Hohlraum Radiation. *Phys. Rev. Lett.* **92**, 85002-1–4.

Boercker, D.B., Iglesias, C.A. & Dufty, J.W. (1987). Radiative and transport properties of ions in strongly coupled plasmas. *Phys. Rev.* **36**, 2254–2264.

Brissaud, A., Goldbach, C., Leorat, J., Mazure, A. & Nollez, G. (1976). On the validity of the model microfield method as applied to Stark broadening of neutral lines. *J. Phys. B* **9**, 1129–1146; Application of the model microfield method to Stark profiles of overlapping and isolated neutral lines. *ibid* 1147–1162.

Busquet, M., Klapisch, M. & Bar-Shalom, A. (2003). Absorption and emission proiles of unresolved arrays near local thermodynamic equilibrium. *J.Q.S.R.T.* **81**, 255–263.

Busquet, M., Weaver, J.L., Colombant, D.G., Mostovych, A.N., Feldman, U., Klapisch, M., Seely, J.F. & Holland, G. (2004). Absolute x-ray emission of CH plasma created with the Nike laser. In *Spectral Line Shapes* (E. Dalimier, Ed.), pp. 246–253. Paris: Frontier Group.

Cai, M.X., Ishii, I., Clifford, R.H., Montaser, A., Palmer, B.A. & Layman, L.R. (1994). Fundamental properties of helium inductively coupled plasmas measured by high-resolution Fourier transform spectrometry. *Spectrochim. Acta B* **49**, 1081–1095.

Chambers, D.M., Pinto, P.A., Hawreliak, J., Al'Miev, I.R., Gouveia, A., Sondhauss, P., Wolfrum, E., Wark, J.S., Glenzer, S.H., Lee, R.W., Young, P.E., Renner, O., Marjoribanks, R.S. & Topping, S. (2002). K-shell spectroscopy of an independently diagnosed uniaxially expanding laser-produced aluminum plasma. *Phys. Rev. E* **66**, 026410-1–16.

Demura, A.V. & Sholin, G.V. (1975). Theory of Hydrogen Lines Stark Profiles Asymmetry in Dense Plasmas. *J.Q.S.R.T.* **15**, 881–899.

Demura, A.V., Gilles, D. & Stehlé, C. (1995). Comparative Study of Microfield Nonuniformity in Plasmas. *J.Q.S.R.T.* **54**, 123–136.

Demura, A.V. & Gilles, D. (2004). Overview of Plasma Microfield in Stark Broadening of Spectral Lines. In *Spectral Line Shapes* (E. Dalimier, Ed.), pp. 121–128. Paris: Frontier Group.

Ferri, S., Calisti, A., Mosse, C. & Talin, B. (2004). Correlation Effects in Warm and dense Plasmas: Influence of Electron Broadening on Hydrogen Lines. In *Spectral Line Shapes* (E. Dalimier, Ed.),pp. 454–456. Paris: Frontier Group.

Frisch, U. & Brissaud, A. (1971). Theory of Stark broadening—I. Soluble scalar model as a test. *J.Q.S.R.T.* **11**, 1753–1756; Theory of Stark broadening—II. Exact line profile with model microfields. *ibid* 1767–1783.

Fujimoto, T. & Kazansky, S.A. (1997). Plasma polarization spectroscopy. *Plasma Phys. Control. Fusion* **39**, 1267–1294.

Gasparian, P.D., Gerasimov, V.M., Sratostin, A.N., Suvorov, A.E. (1994). Effect of plasma microfields on the gain of hydrogen-like ions with photoresonant pumping. *Zh. Exp. i Teor. Fiziki* **105**, 1593–1605 (1994. *JETP* **78**, 858).

Gigosos, M.A. & Cardenoso, V. (1996). New plasma diagnosis tables of hydrogen Stark broadening including ion dynamics. *J. Phys.* **B 29**, 4795–4838.

Gigosos, M.A., Gonzalez, M.A. & Cardenoso, V. (2003). Computer simulated Balmer-alpha, -beta and -gamma Stark line profiles for non-equilibrium plasmas diagnostics. *Spectrochimica Acta* **Part B 58**, 1489–1504.

Gilles, D. (1990). Analytical fit of MonteCarlo distribution s of the electric microfield in a plasma. *Ann. Phys. Colloq. France* **15**, C3, 85–87

Gilles, D. & Stehlé, C. (1994). Application of the Model Microfield Method to the Stark Broadening of Ions. *Laser Part. Beams* **12**, 413–420.

Gilles, D. & Stehlé, C. (1995). Line Shapes of Multiply-charged Ions: Ion Dynamics and Concentration Effects. *J. Phys. II France* **5**, 75–92.

Golovkin, I., Mancini, R.C., Louis, S., Ochi, Y., Fujita, K., Nishimura, H., Shirga, H., Miyanaga, N., Azechi, H., Butzbach, R., Uschmann, I., Föerster, E., Delettrez, J., Koch, J., Lee, R.W. & Klein, L. (2002). Spectroscopic Determination of Dynamic Gradients in Implosion Cores. *Phys. Rev. Lett.* **88**, 04502-1–4.

Gouveia, A., Al'miev, I.R., Hawreliak, J., Chambers, D.M., Liang, T., Marjoribanks, R., Pinro, P.A., Renner, O., Zhang, J. & Wark, J.S. (2003). Absorption spectroscopy of Al XIII Ly-α radiation by an Fe XXIV plasma. *J.Q.S.R.T.* **81**, 199–207.

Griem, H.R. (1974). *Spectral Line Broadening by Plasmas*. New York: Academic Press.

Grützmacher, K. & Wende, B. (1977). Discrepancies between the Stark broadening theories of hydrogen and measurements of Ly-α Stark profiles in a dense equilibrium plasmas. *Phys. Rev. A* **16**, 243–246.

Hakel, P., Mancini, R.C., Gauthier, J.-C., Minguez, E., Dubau, J. & Cornille, M. (2004). X-ray line polarization of He-like Si satellite spectra in plasmas driven by high-intensity ultrashort pulsed lasers. *Phys. Rev. E* **69**, 056405-1-11.

Hammarsten, E.C., Szapiro, B., Jankowska, E., Filevich, J., Marconi, M.C. & Rocca, J.J. (2004). Soft X-ray laser diagnostics of exploding aluminum wire plasmas. *Appl. Phys. B* **78**, 933–937.

Hasegawa, J., Yokoya, N., Kobayashi, Y, Yoshida, M., Kojima, M., Sasaki, T., Fukuda, H., Ogawa, M., Oguri, Y. & Murakami, T. (2003). Stopping power of dense helium plasma for fast heavy ions. *Laser Part. Beams* **21**, 7–11.

Holtsmark, J. (1919). The broadening of spectral lines. *Ann. Physik* **58**, 577–630.

Iglesias, C.A., Rogers, F.J., Shepherd, R., Bar-Shalom, A., Murillo, M.S., Kilcrease, D.P., Calisti, A. & Lee, R.W. (2000). Fast electric microfield distribution calculations in extreme matter conditions. *J.Q.S.R.T.* **65**, 303–315.

Inglis, D.R. & Teller, E. (1939). Ionic Depression of Series Limits in One-Electron Spectra. *Astroph. J.* **90**, 439–448.

Kepple, P. & Griem, H.R. (1968). Improved Stark Profile Calculations for the Hydrogen Lines Hα, Hβ, Hγ, and Hδ. *Phys. Rev.* **173**, 317–325.

Kilcrease, D.P., Mancini, R.C. & Hooper, C.F., Jr. (1993). Ionic broadening of dense plasma spectral lines including field-dependent atomic physics and the ion quadrupole interaction. *Phys. Rev E* **48**, 3901–3913.

Koenig, M., Malnoult, Ph. & Nguyen, H. (1988). Atomic structure and line broadening of He-like ions in hot and dense plasmas. *Phys. Rev. A* **38**, 2089–2098.

Kosarev, I.N., Stehlé, C., Feautrier, N., Demura, A.V. & Lisitsa, V.S. (1997). Interference of radiating states and ion dynamics in spectral line broadening. *J. Phys. B. At. Mol. Phys.* **30**, 215–236.

Langer, S.H., Scott, H.A., Marinak, M.M. & Landen, O.L. (2003). Comparisons of line emission from 2- and 3-dimensional simulations of ICF capsules to experiments. *J.Q.S.R.T.* **81**, 275–286.

Leboucher-Dalimier, E., Sauvan, P., Angelo, P., Poquérusse, A., Schott, R., Dufour, E., Minguez, E. & Calisti, A. (2001). Observation of ion-ion correlation effects on emissivity and opacity of hot ultra-dense low Z plasmas. *J.Q.S.R.T.* **71**, 493–504.

Loboda, P.A., Litvinenko, I.A., Baydin, G.V., Popova, V.V. & Koltchugin, S.V. (2000). Line shape modeling of multielectron ions in plasmas. *Laser Part. Beams* **18**, 275–289.

Magunov, A.I., Faenov, A.Ya., Skobelev, I.Yu., Pikuz, T.A., Dobosz, S., Schmidt, M., Perdrix, M., Meynadier, P., Gobert, O., Normand, D., Stenz, C., Bagnoud, V., Blasco, F., Roche, J.R., Salin, F. & Sharkov, B. Yu. (2003). X-ray spectra of fast ions generated from clusters by ultrashort laser pulses. *Laser Part. Beams* **21**, 73–79.

Mathys, G., Stehlé, C., Brillant, S. & Lanz, T. (2000). The physical foundations of stellar magnetic field diagnosis from polarimetric observations of hydrogen lines. *Astron. Astrophys.* **358**, 1151–1156.

Nguyen, H., Koenig, M., Benredjem, D., Caby, M. & Coulaud, G. (1986). Atomic structure and polarization line shift in dense and hot plasmas. *Phys. Rev. A* **33**, 1279–1290.

Oks, E. (1995). *Plasma Spectroscopy: The Influence of Microwave and Laser Fields*. New York: Springer.

Politov, V.Yu., Potapov, A.V. & Antonova, L.V. (2000). About diagnostics of *Z*-pinches hot points. *Laser Part. Beams* **18**, 291–296.

Potekhin, A.Y., Chabrier, G. & Gilles, D. (2002). Electric microfield distributions in electron-ion plasmas. *Phys. Rev. E* **65**, 036412-1-12.

Rautian, S.G. & Shalagin, A.M. (1991). *Kinetic Problems of Non-Linear Spectroscopy*. New York: North Holland.

Regan, S.P., Delettrez, J.A., Marshall, F.J., Soures, J.M., Smalyuk, V.A., Yaakobi, B.R., Epstein, R., Glebov, V.Yu, Jaanimagi, P.A., Meyerhofer, D.D., Radha, P.B., Sangster, T.C., Seka, W., Skupsky, S., Stoeckl, C., Town, R.P.J., Haynes, D.A., Jr., Golovkin, I.E., Hooper, C.F., Jr., Frenje, J.A., Li, C.K., Petrasso, R.D. & Seguin, F.H (2002). Shell Mix in the Compressed Core of Spherical Implosions. *Phys. Rev. Lett.* **89**, 085003-1-4.

Renner, O., Limpouch, J., Krousky, E., Uschmann, I. & Föerster, E. (2003). Spectroscopic characterization of plasma densities of laser-irradiated Al foils. *J.Q.S.R.T.* **81**, 385–394.

Rosmej, F.B., Calisti, A., Stamm, R., Talin, B., Moss, C., Ferri, S., Geibel, M, Hofmann, D.H.H., Faenov, A.Ya. & Pikuz, T.A. (2003). Strongly coupled laser produced plasmas: investigation of hollow ion formation and line shape analysis. *J.Q.S.R.T.* **81**, 395–409.

Seidel, J. (1977). Hydrogen Stark Broadening by Model Electronic Microfields. *Z. für Naturforschung* **32a**, 1195–1206; Effects of Ion Motion on Hydrogen Stark Profiles. *ibid* 1207–1214.

Stamm, R., Pollock, E.L., Talin, B. & Iglesias, C.A. (1986). Ion dynamics effects on the line shapes of hydrogenic emitters in plasmas. *Phys. Rev. A* **34**, 4144–4152.

Stehlé, C. (1990). What means low or high densities for Stark broadening of hydrogenic ions lines? *J.Q.S.R.T* **44**, 135–142.

Stehlé, C. & Hutcheon, R. (1999). Extensive tabulations of

Stark broadened hydrogen line profiles. *Astron. Astrophys. Suppl. Ser.* **140**, 93–97.

Stehlé, C., Gilles, D. & Demura, A.V. (2000). Asymmetry of Stark profiles: The microfield point of view. *Eur. Phys. J*. D **12**, 355–367.

Stygar, W.A., Ives, H.C., Fehl, D.L., Cuneo, M.E., Mazarakis, M.G., Bailey, J.E., Bennett, G.R., Bliss, D.E., Chandler, G.A., Leeper, R.J., Matzen, M.K., McDaniel, D.H., McGurn, J.S., McKenney, J.L., Mix, L.P., Muron, D.J., Porter, J.L., Ramirez, J.J., Ruggles, L.E., Seamen, J.F., Simpson, W.W., Speas, C.S., Spielman, R.B., Struve, K.W., Torres, J.A., Vesey, R.A., Wagoner, T.C., Gilliland, T.L., Horry, M.L., Jobe, D.O., Lazier, S.E., Mills, J.A., Mulville, T.D., Pyle, J.H., Romero, T.M., Seamen, J.J. & Smelser, R.M. (2004). X-ray emission from *z* pinches at 10^7 A: Current scaling, gap closure, and shot-to-shot fluctuations. *Phys. Rev. E* **69**, 046403-1-20.

Talin, B., Calisti, A., Godbert, L., Stamm, R., Lee, R.W. & Klein, L. (1995). Frequency-fluctuation model for line-shape calculations in plasma spectroscopy. *Phys. Rev*. A **51**, 1917–1928.

Talin, B., Dufour, E., Calisti, A., Gigosos, M.A., Gonzalez, M.A., Del Rio Gaztelurrutia, T. & Dufty, J.W. (2003). Molecular dynamics simulation for modelling plasma spectroscopy. *J. Phys. A* **36**, 6049–6056.

Underhill, A.B. & Waddell, J.H. (1959). Stark Broadening Functions for the Hydrogen Lines. NBS Circular 603.

Vinogradov, A.V., Sobelman, I.I. & Yukov, E.A. (1974). On Spectroscopic Methods for Superdense Hot Plasmas Diagnostics. *Quantum Electronics* **1**, 268 (in Russian).

Vidal, C.R., Cooper, J. & Smith, E.W. (1973). Hydrogen Stark-Broadening Tables. *Astrophys. J. Suppl. Ser.* **25**, 37–136.

Welser, L.A., Mancini, R.C., Koch, J.A., Izumi, N., Dalhed, H., Scott, H., Barbee, T.W., Jr., Lee, R.W., Golovkin, I.E., Marshall, F., Delettrez, J. & Klein, L. (2003). Analysis of the spatial structure of inertial confinement fusion implosion cores at OMEGA. *J.Q.S.R.T.* **81**, 487–497.

Woolsey, N.C., Hammel, B.A., Keane, C.J., Back, C.A., Moreno, J.C., Nash, J.K., Calisti, A., Mossé, C., Godbert, L., Stamm, R., Talin, B., Hopper, C.F., Jr., Asfaw, A., Klein, L. & Lee, R.W. (1997). Evolution of electron temperature and electron density in indirectly driven spherical implosions. *Phys. Rev. E* **56**, 2314–2317.

Ying, M.J., Xia, Y.Y., Sun, Y.M., Zhao, M.W., Ma, Y.C., Liu, X.D., Li, Y.F. & Hou, X.Y. (2003). Plasma properties of a laser-ablated aluminum target in air. *Laser Part. Beams* **21**, 97–101.

Zeitoun, P., Balcou, P., Bucourt, S., Delmotte, F., Dovillaire, G., Douillet, D., Dunn, J., Faivre, G., Fajardo, M., Goldberg, K.A., Hubert, S., Hunter, J.R., Idir, M., Jacquemot, S., Kazamias, S., Le Pape, S., Levecq, X., Lewis, C.L.S., Marmoret, R., Merceren, P., Morlens, A.S., Naulleau, P.P., Ravet, M.F., Remond, C., Rocca, J.J., Smith, R.F., Troussel, P., Valentin, C. & Vanbostal, L. (2004). Recent developments in X-UV optics and X-UV diagnostics. *Appl. Phys. B* **78**, 983–988.